

Intrinsic resonant behavior of metamaterials by finite element calculations

Abdelilah Mejdoubi and Christian Brosseau*

Département de Physique, Université de Bretagne Occidentale, CS 93837, 6 avenue Le Gorgeu, 29238 Brest Cedex 3, France

(Received 25 July 2006; revised manuscript received 7 August 2006; published 27 October 2006)

We report on computer based simulations of multiple electrostatic resonances (ER) of two-dimensional metamaterials with various shape including fractal structures, complex permittivity of the inclusion, and composition. Our model structures are made of inclusions of materials with the negative real part of the permittivity in a dielectric host with positive permittivity. Remarkably, our simulations which are based on a finite-element method without use of the dipole approximation indicate that in the vicinity of an intrinsic ER, i.e., independent of the spectral material properties of the inclusion, the effective permittivity of the heterostructure depends sensitively on the dielectric object shape, allowing its magnitude and sign to be tuned to any value. Two unique features of the ER are found: these resonances become broader and weaker as the losses are increasing, and the associated local fields of such resonances exhibit strong enhancements in small parts of the structure.

DOI: [10.1103/PhysRevB.74.165424](https://doi.org/10.1103/PhysRevB.74.165424)

PACS number(s): 78.20.Ci, 41.20.Cv, 42.70.Qs, 78.66.-w

In recent years there has been a focus on developing artificially fabricated structures that exhibit unique properties not found in nature, e.g., metamaterials,¹ photonic crystals (PC) (Ref. 2). Although several unusual characteristics have already been envisioned and even demonstrated, several questions remain pertaining to the response of these structures to an incident electromagnetic radiation. On the other hand, interest has accelerated in the last few years in the unique properties of electrostatic resonances (ER) as new method to characterize the electromagnetic properties of periodic nanostructures (see, for example, Ref. 3, and references therein). These ER result in very strong and localized electric fields. ER studies⁴ have drawn a lot of attention due to their possible applications to subwavelength imaging, negative refractive index optics, and plasmon-polariton circuits. In a recent work,⁴ Fredkin and Mayergoyz demonstrated that the resonance values of ε can be directly found by computing the eigenvalues of a specific boundary integral equation.

Consider a general two-dimensional (2D) two-phase system which can be defined as a bounded domain in \mathbb{R}^2 of surface Ω which has effective permittivity ε , in which there is no source charge. Solving the problem at hand means finding expressions for the scalar potential V and electric field $\mathbf{E} = -\nabla V$ everywhere within the domain Ω . The occurrence of ER is a common feature of inhomogeneous composite materials. From the basic physics point of view, ER are defined as eigenstates of the electric potential problem, i.e., find nontrivial solutions $V(\mathbf{r})$ of the Laplace partial differential equation, $\nabla \cdot [\varepsilon(\mathbf{r}) \nabla V(\mathbf{r})] = 0$ that vanish on the surface of the composite, where $\varepsilon(\mathbf{r})$ and $V(\mathbf{r})$ are the local permittivity and potential inside Ω , respectively.^{7,8} Suppose for simplicity that the mixed medium consists of two isotropic phases, each of which is characterized by a scalar permittivity ε_i . An important example that we consider below is the periodic assemblage of constituent two embedded in a host of constituent one, with respective surface fraction ϕ_2 and $1 - \phi_2$.

A distinction between intrinsic and extrinsic resonant behavior arises when the effects of geometry of the polarizable inclusion and frequency dependent permittivity $\varepsilon_2(\omega)$ are considered separately. For a given assemblage of inclusions,

the ER is intrinsic, i.e., independent of the model assumption for the functional dependence $\varepsilon(\omega)$, and is distinguished by the extrinsic ER for which the appropriate frequency dependent permittivity should be employed to find the resonance modes. Until presently, the only known physical (extrinsic) characterization of ER involved different kinds of functional dependence of $\varepsilon_2(\omega)$, e.g., plasma permittivity with $\varepsilon_2(\omega) = 1 - \omega_p^2/\omega^2$ (Refs. 3 and 4), and polaritonic behavior $\varepsilon_2(\omega) = \varepsilon_\infty(\omega^2 - \omega_{LO}^2)/(\omega^2 - \omega_{TO}^2)$, with $\varepsilon_2 < 0$ for $\omega_{TO} < \omega < \omega_{LO}$.⁹ The main question surrounding the calculation of negative values of ε centers around the general physical properties of intrinsic ER.

The motivation for this study comes from two points of view. One is the early suggestion¹⁰ of Bergman and Milton (BM) that a modal formalism permits to separate the effect of the dielectric properties of the constituent materials from the effect of the geometry of a two-component composite. Appropriately, BM appreciated the fact that the effective properties are given by an integral transform of a function that depends only on the geometry of the composite and are independent of the specific material properties of the inclusions.¹⁰ However, this partial-differential eigenvalue problem cannot be efficiently solved for irregular inclusion shapes. In view of the simplicity and robustness of the method both in 2D and three-dimensional (3D) complex geometries, a finite-element (FE) type of computation presents itself as the natural tool for numerics. Another line of work, initiated recently,^{5,6} made in relation to small 2D and 3D objects of arbitrary shape showed that the polarization behavior possesses intrinsic properties which may be vital in guiding the rational design of metamaterials and PC.

With this in mind, the main goal in this paper is to report the results of investigations on the intrinsic ER of negative-permittivity media by using a procedure based on the FE method and similar to that of Ref. 11, that allows for the generation of data for inclusion shapes that are not amenable to analytic methods. In the remainder of this paper, FE simulations, as implemented in the Comsol multiphysics simulation package,¹² are used to show that by changing the composition of 2D structures, in the vicinity of an ER, ε depends sensitively on the complex permittivity ε_2 and on the assem-

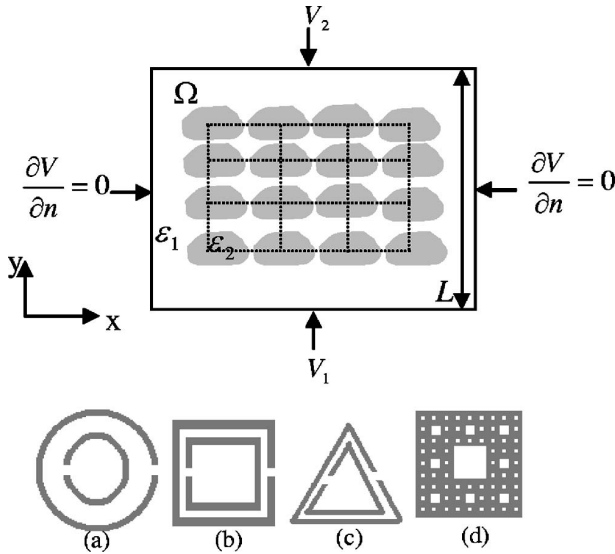


FIG. 1. The higher panel shows the cartoon sketch of the unit square cell in the (x, y) plane of a typical 2D composite structure containing the inclusion (shaded region). The model space can simulate a capacitor by applying a potential difference between the top and bottom faces of the model space. The evaluation of the effective permittivity, along the direction corresponding to the applied field, i.e., $\varepsilon = \varepsilon_y$, requires that the conservation of the electric displacement flux through the “surface” S has to be solved subject to appropriate the relevant boundary conditions for the potential. We fix $V_1 = 0$ V and $V_2 = 1$ V and assume that $\frac{\partial V}{\partial n} = 0$ on the other side faces. L and S have both been set to unity. The lower panel contains the structural motif of the isolated inclusions: (a) split-ring (SR), (b) split-square (SS), (c) split-triangle (ST), (d) Sierpinski square (3rd iteration).

blage of inclusions allowing the magnitude and sign of ε to be tuned to any value. We hope that the structural characteristics of ER can be used as a theoretical tool to classify wave transport behavior in artificial structures (metamaterials and PC) that exhibit a tunable electromagnetic response. An important point to emphasize is that, unlike the known functional dependences mentioned above, the present results are independent of $\varepsilon_2(\omega)$. It will be shown that these metamaterials can support localized electric field enhancement in small parts of the structure. The distribution of the local electric field is of great fundamental and practical importance in the study of heterogeneous material because: (i) the effective permittivity is determined from lower moments of the local field, and (ii) it is fundamental to understanding failure or breakdown phenomena.

Current work within this research group focuses on the use of various systematic and versatile procedures for calculating the effective (relative to the permittivity of a vacuum) permittivity of mixed media based on numerical methods.^{11,13,14} The upper panel of Fig. 1 provides an illustration of the equivalent parallel-plate capacitor. When there is an adequate separation of scales between sizes of inclusion and of the overall composite we can characterize the dielectric behavior with an effective permittivity. The calculation of the effective permittivity of composite structures proceeds as follows. (1) The space is a unit square containing elementary

cells using a grid of points whose sharpness enables a good approximation of the contour of the spatial domain Ω . The space is filled with the desired arrangement, i.e., the permittivities of the cells are set equal to ε_1 or ε_2 depending on whether the cell is filled with phase 1 or phase 2, respectively. (2) The local potential distribution inside Ω which has no free charges or currents is given by the conservation of electric displacement flux through the “surface” S .¹³ In our case, the effective permittivity along the direction corresponding to the applied field, i.e., $\varepsilon = \varepsilon_y$, is found by integration via $\int_S \varepsilon_1 \left(\frac{\partial V}{\partial n} \right)_1 = \varepsilon \frac{V_2 - V_1}{L} S$, where $V_2 - V_1$ denotes the difference of potential imposed in the y direction, L is the composite thickness in the same direction, and S is the “surface” of the unit cell perpendicular to the applied field. The potential on the top face of the square, V_2 , is fixed at a value of 1 V, while that on the bottom face, V_1 , is fixed at 0 V. (3) It is worth observing that the fully automatic generation of high quality meshes plays a crucial role in the finite element analysis, influencing both ease of use and accuracy of a software package. In the FE method, the domain can be discretized into a number of uniform or nonuniform finite-elements that are connected via nodes. The change of V with regard to spatial position is approximated within each element by an interpolation function. The original boundary value problem is then replaced with an equivalent integral formulation. The interpolation functions are then substituted into the integral equation, integrated, and combined with the results from all other elements in the domain Ω . Then, the results of this procedure are transformed into a matrix equation which is subsequently solved for V .

For simplicity, we will focus our discussion on 2D deterministic two-phase heterostructures. In all cases, the simulation cell Ω is a square of length $L = 1$. As a side note, we do point out that we verified that if one of the two dimensions of the simulation box is significantly longer than the other one, e.g., rectangular cell (1×2) instead of the unit square cell, does not influence the permittivity and depolarization factor values. Periodic boundary conditions are enforced in the x direction for these structures. All data were obtained using the FE element as implemented in the commercial finite-element solver Comsol Multiphysics® and the procedure sorted out ε on a personal computer with a Pentium IV processor (3 GHz). The field calculation package Comsol MultiPhysics® permits the closely controlled generation of finite-element meshes through the use of input files containing complete instructions for node-by-node and element-by-element mesh specifications, along with imposition of the boundary conditions on each side of the unit cell as displayed in the upper panel of Fig. 1. One basic question is as follows: How can the number of nodes in the mesh affect the quality of the obtained results? We tested coarse meshes with meshes of increasing fineness and found that above a mesh size of a few thousand elements the numerical results for the permittivity were constant and reproducible. For the numerical solution we discretized the configuration investigated here with a number of elements ranging between 5000 and 10 000, which means a linear system of equations with typically 20 000 unknowns has to be solved. We refer the reader to Refs. 11 and 13 for full details on the merits and the implementation of the algorithm.

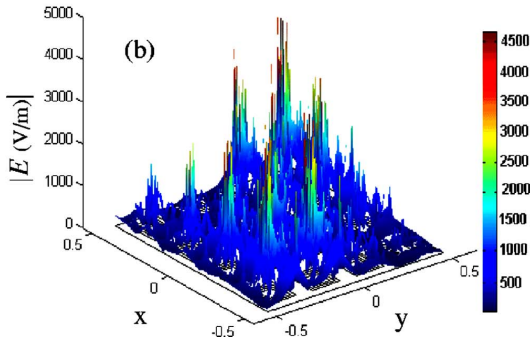
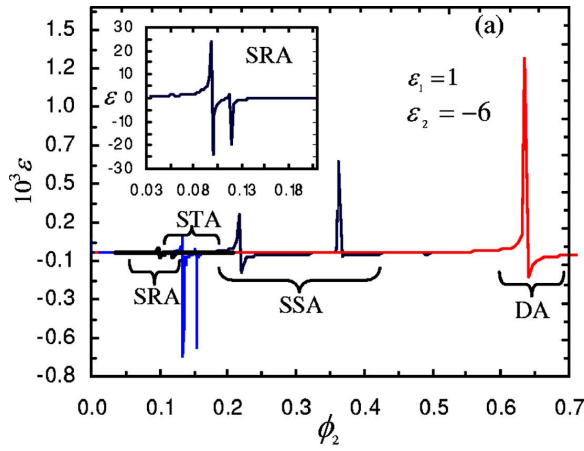


FIG. 2. (a) (Color online) The dependence of the effective permittivity ϵ of 4×4 square arrays of lossless split inclusions ($\epsilon_2 = -6$) in a host matrix ($\epsilon_1 = 1$) as a function of the surface fraction of inclusion. Split-inclusions considered are: the blue (black) curves are for split-ring (SRA), split-triangle (STA), and split-square (SSA). For the purpose of comparison, we have also indicated in red (gray) the case of square array of disks (DA). The inset shows an expanded view of the region around $\phi_2 = 0.1$ for SRA. (b) Electric field norm distribution of resonance mode for the 2D composite structure composed of a 4×4 SSA. $\phi_2 = 0.217$. The color bar indicates the norm scale in Vm^{-1} unit.

While strictly valid only in a dc situation, in fact these calculations can be extended to nonzero frequencies. Within the quasistatic assumption (QA), ϵ acquires a nonzero imaginary part and the real part may violate the dc requirement of positivity for ϵ . By quasistatic we imply that all inhomogeneity length scales should be small compared to the electromagnetic wavelength λ of the radiation probing the system and to the skin depth. We discuss two basic kinds of inhomogeneities: (i) square lattices of split-inclusions, and (ii) square arrays of deterministic fractal inclusions. The inclusions under consideration are shown in the lower panel of Fig. 1. Observe that lattice arrays of conducting dual split-ring resonators were used by Smith *et al.*¹ first demonstration of metamaterials with negative permittivity and magnetic permeability.

First the general features observed in the simulations are described. In Fig. 2(a) we display our numerically computed values of ϵ for a selection of 4×4 square arrays of lossless inclusions. There are several remarkable features visible in Fig. 2(a). First of all, it is worth noting the asymmetry shape of the ER peaks. Another important aspect about ER drawn

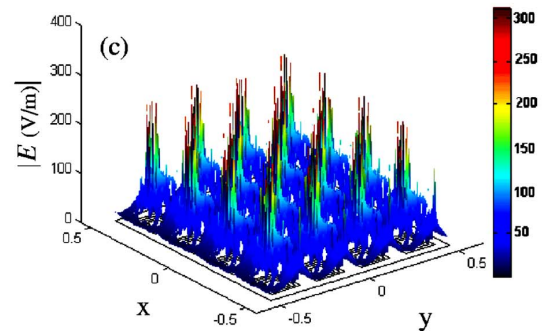
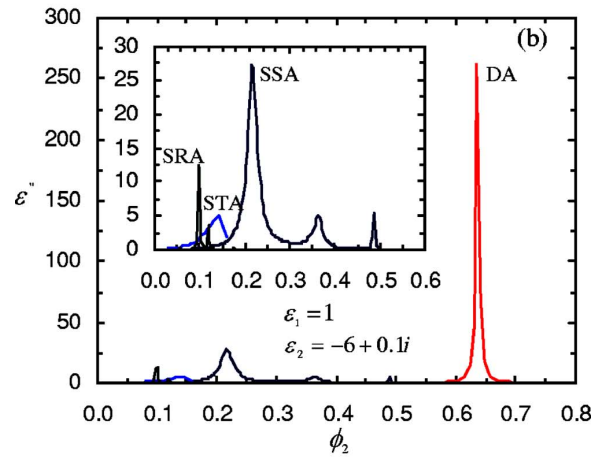
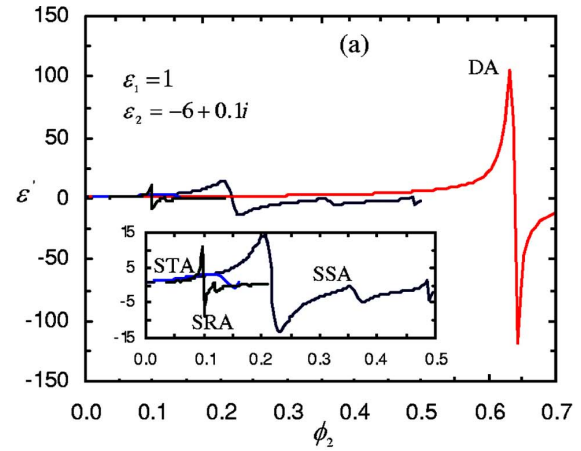


FIG. 3. (Color online) Same as in Fig. 2 for lossy inclusions ($\epsilon_2 = -6 + 0.1i$). The inset shows an expanded view of the region from $\phi_2 = 0$ to $\phi_2 = 0.5$ for SRA, SSA, and STA. (a) Real part of ϵ ; (b) imaginary part of ϵ . (c) Electric field norm distribution of resonance mode for the 2D composite structure composed of a 4×4 SSA. $\phi_2 = 0.217$. The color bar indicates the norm scale in Vm^{-1} unit.

from this figure is the ordered progression of the ER when ϵ is plotted as function of ϕ_2 ; the surface fraction for the ER of split-ring array (SRA) is six times smaller than that for the DA. Note that the pair of peaks observed for split-inclusions does not mean that the mode is doubly degenerated but is related to the two separate parts of the double split-inclusions. Auxiliary simulations (not shown) showed that the ER peak is shifted when ϵ_2 is changed. For example, choosing $\epsilon_2 = -7$ we found that ER occurs at $\phi_2 = 0.318$ for

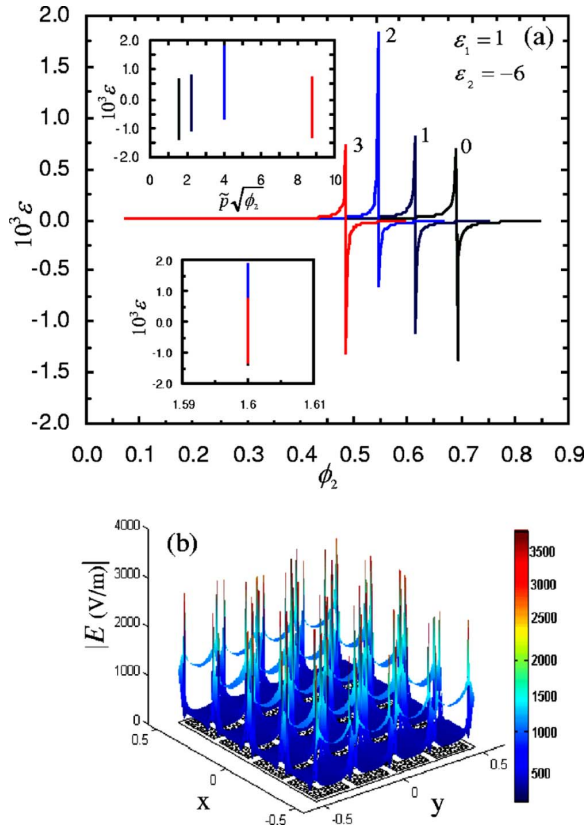


FIG. 4. (a) (Color online) The dependence of the effective permittivity ε of square arrays of fractal (Sierpinski square) lossless inclusions ($\varepsilon_2 = -6$) in a host matrix ($\varepsilon_1 = 1$) as a function of the surface fraction of inclusion. The colors and numbers denote the different iterations of the fractal inclusion. The upper inset shows the same data as in (a) but now they are plotted as a function of $\tilde{p}\sqrt{\phi_2}$. The lower inset shows the data collapse using the similarity transformation; (b) Electric field norm distribution of resonance mode for the 2D composite structure composed of a 4×4 Sierpinski square. (The parameters are $\phi_2 = 0.484$, third iteration.) The color bar indicates the norm scale in Vm^{-1} unit.

split-square array (SSA). In Fig. 2(b) we show the local electric field norm $|\mathbf{E}(\mathbf{r})|$ associated with the resonant mode $\phi_2^{(\text{SSA})} = 0.217$. This plot indicates that the strongest electric field enhancements are found in small parts of the planar composite.

Now we turn to the ER for the corresponding lossy structures. Comparing the ER with the lossless case, we see a striking difference in the line shapes as illustrated in Figs. 3(a) and 3(b): While for the lossless inclusion the ER is narrow, for the lossy inclusion the ER is broadened and attenuated. However, the ER for both lossless and lossy structures occur at the same surface fraction. Importantly, the ER peaks display a significant symmetry in contrast with the asymmetry which is clearly visible in Fig. 2(a). It is interesting to note that even small material losses can have a strong impact on the ER characteristics. A larger imaginary part of ε_2 causes a stronger broadening and a reduction of intensity (not shown). As shown in Fig. 3(c), the electric field norm map vs x and y shows a very different behavior from the previous lossless case. In addition, the fourfold symmetry of

the map is evident from this figure. Comparing panels (b) in Fig. 2 and (c) in Fig. 3, we conclude that the ER line broadening for lossy inclusions is associated with a one order of magnitude decrease of the electric field norm.

In the course of analyzing the polarization properties of perforated 2D structures, the authors^{6,11} developed a deterministic fractal modeling for shape functional of voided structures. Figure 4(a) shows the result of ε calculation for 4×4 square array of Sierpinski squares. The main features of this plot are the asymmetry of the ER peaks and the shift of the ER towards lower surface fraction as the iteration number of the structure is increased. Recently, it was reported that the $\tilde{p}\sqrt{\phi_2}$ dependence of ε provides us with a simple means to rationalize the dielectric behavior as the number of iteration of the fractal pattern changes, where the reduced perimeter is $\tilde{p} = \frac{P}{K}$, with P and K being the perimeter and the surface area of the fractal pattern, respectively.⁶ Most notable was our observation that the ε vs $\tilde{p}\sqrt{\phi_2}$ of these structures can be modeled according to the similarity transformation $\varepsilon_0(\tilde{p}_0\sqrt{\phi_{20}}) = \varepsilon_n[s(n)(\tilde{p}_n\sqrt{\phi_{2n}})]$, where ε_n is the permittivity for iteration number n and

$$s(n) = 5(8^{n/2}/4(3^n) + 8^n)$$

for a Sierpinski square. As indicated by this similarity transformation, the behavior of the permittivity vs iteration number of the fractal structure can be used to obtain a single master curve. This inference is confirmed on the graph of the lower inset of Fig. 4(a), where the collapse of data in a single graph indicates that the similarity transformation holds quite well at least for the first three iterations. The highest ER surface fraction, $\phi_2 \approx 0.7$, corresponds to the primitive square (iteration zero) for the Sierpinski square. By comparing the real and imaginary parts of ε , calculated in the same condition, we also found that with increasing the inclusion losses, the ER is significantly broadened and attenuated (not shown).

We now turn to a discussion of two main points. As for the first point, our FE simulations establish that the dependence $\varepsilon(\phi_2)$ cannot be understood by considering a dipolar description, e.g., Maxwell Garnett, since the dipolar approximation^{7,15} is only valid if the unit cell $\ll \lambda$ and if the exciting field is homogeneous across the dimensions of the inclusion. Obviously, the strong spatial fluctuations of the local-field seen in Figs. 2(b), 3(c), and 4(b) imply that the latter requirement is violated. In that case the depolarizing factor is modified by the presence of structurally induced multipoles.^{7,11,16} As for the second point addressed in this paper, the FE simulations were motivated by the fact that evaluation of intrinsic ER does not require that we know $\varepsilon_2(\omega)$, insofar as the continuum QA is valid. Aside from a few general considerations given above, this function depends in detail upon the modes carrying electromagnetic energy. However, except for somewhat simple artificial materials, this function cannot be easily determined analytically. This issue is particularly relevant to nanophases for which ε_2 is a local complex function of frequency which may strongly differ from its bulk value.

To summarize, we have developed a numerical description of ER of metamaterials of complex shapes. They illus-

trate the statement that the ER which is an intrinsic property of object shapes displays a rich variety of behavior that provide a fertile ground for characterizing the interaction of a polarizable negative-permittivity medium with an incident electromagnetic radiation. Our simulations provide a possibility for detailed investigation of the interplay between the spatial pattern and the distribution of the local electric field, i.e., fluctuations of the local field. It turns out that, independent of exact form of the functional $\varepsilon_2(\omega)$, intrinsic ER lies within a narrow range of surface fraction, whereas lossy inclusions show a much broader ER. The method proves to be

of sufficient generality in that it allows for estimations of ER arising from the interaction of dielectric objects possessing polarizabilities of arbitrary electric multipole moment order, offering an alternate calculational approach than the BM formulation.

ACKNOWLEDGMENTS

This work was supported by the Laboratoire d'Electronique et Systèmes de Télécommunications, Unité Mixte de Recherche CNRS 6616.

*Electronic address: brosseau@univ-brest.fr

- ¹See, e.g., D. R. Smith, J. B. Pendry, and M. C. K. Wiltshire, *Science* **292**, 77 (2004); **305**, 788 (2004); J. Zhou *et al.*, *Phys. Rev. Lett.* **95**, 223902 (2005); W. J. Padilla, A. J. Taylor, C. Highstrete, M. Lee, and R. D. Averitt, *ibid.* **96**, 107401 (2006).
²E. Yablonovitch, *Phys. Rev. Lett.* **58**, 2059 (1987); S. John, *ibid.* **58**, 2486 (1987).
³G. Shvets and Y. A. Urzhumov, *Phys. Rev. Lett.* **93**, 243902 (2004).
⁴D. R. Fredkin and I. D. Mayergoyz, *Phys. Rev. Lett.* **91**, 253902 (2003); I. D. Mayergoyz, D. R. Fredkin, and Z. Zhang, *Phys. Rev. B* **72**, 155412 (2005).
⁵E. J. Garboczi and J. F. Douglas, *Phys. Rev. E* **53**, 6169 (1996); M. L. Mansfield, J. F. Douglas, and E. J. Garboczi, *ibid.* **64**, 061401 (2001); J. F. Douglas and E. J. Garboczi, *Adv. Chem. Phys.* **91**, 85 (1991).
⁶A. Mejdoubi and C. Brosseau, *Phys. Rev. E* **73**, 031405 (2006).
⁷D. J. Bergman and D. Stroud, *Solid State Phys.* **46**, 147 (1992); M. I. Stockman, S. V. Faleev, and D. J. Bergman, *Phys. Rev.*

- Lett.* **87**, 167401 (2001).
⁸G. W. Milton, *The Theory of Composites* (Cambridge University Press, Cambridge, 2002).
⁹M. S. Wheeler, J. S. Aitchison, and M. Mojahedi, *Phys. Rev. B* **72**, 193103 (2005).
¹⁰D. J. Bergman, *Phys. Rev. B* **14**, 4304 (1976); G. W. Milton, *Appl. Phys. Lett.* **37**, 300 (1980).
¹¹A. Mejdoubi and C. Brosseau (to be published).
¹²*Comsol Multiphysics Reference Manual* (Comsol AB, Stockholm, Sweden, 2003).
¹³C. Brosseau and A. Beroual, *Prog. Mater. Sci.* **48**, 373 (2003).
¹⁴V. Myroshnychenko and C. Brosseau, *Phys. Rev. E* **71**, 016701 (2005).
¹⁵W. Lamb, D. M. Wood, and N. W. Ashcroft, *Phys. Rev. B* **21**, 2248 (1980).
¹⁶R. E. Raab and O. L. de Lange, *Multipole Theory in Electromagnetism* (Clarendon, Oxford, 2005).